Used Fuel Disposition Campaign

Engineered Barrier System (EBS) Evaluations
(Work Package FT-12LL080604)

Level 4 Milestone (M4): M4FT-12LL0806041.

FY12 THERMODYNAMIC PROPERTIES REPORT

THERMODYNAMIC DATABASE DEVELOPMENT, WITH EMPHASIS ON COMPLEX CLAY MINERALS -

Lawrence Livermore National Laboratory

Thomas Wolery

MAY 1ST 2012

LLNL-TR-554331

Introduction

Thermodynamic data are essential for understanding and evaluating geochemical processes, as by speciation-solubility calculations, reaction-path modeling, or reactive transport simulation. Such data are required to evaluate both equilibrium states and the kinetic approach to equilibrium (via the affinity term in most commonly used rate laws). The development of thermodynamic databases for these purposes has a long history in geochemistry (e.g., Garrels and Christ, 1965; Helgeson et al., 1969; Helgeson et al., 1978, Johnson et al., 1992; Robie and Hemingway, 1995), paralleled by related and applicable work in the larger scientific community (e.g., Wagman et al., 1982, 1989; Cox et al., 1989; Barin and Platzki, 1995; Binneweis and Milke, 1999). The Yucca Mountain Project developed two qualified thermodynamic databases to model geochemical processes, including ones involving repository components such as spent fuel. The first of the two (BSC, 2007a) was for systems containing dilute aqueous solutions only, the other (BSC, 2007b) for systems involving concentrated aqueous solutions and incorporating a model for such based on Pitzer's (1991) equations . A 25°C-only database with similarities to the latter was also developed for WIPP (cf. Xiong, 2005).

The YMP dilute systems database is widely used in the geochemistry community for a variety of applications involving rock/water interactions. It builds on the work of Prof. Helgeson and his students (see BSC, 2007a for many applicable references), and covers a significant range of temperature (25-300°C). The last version covers 86 chemical elements, 1219 aqueous species, 1156 minerals and other solids species, and 128 gas species. Many data for actinide species were adopted from the Nuclear Energy Agency (NEA) series of volumes on radionuclide element thermodynamics (see references given in BSC, 2007a), and the appropriate temperature extrapolations were applied. The YMP concentrated systems database covers a smaller chemical system (40 chemical elements, 237 aqueous species, 470 minerals and other solids, and 11 gas species). It includes temperature dependence, which for many species extends to 200°C, but for others extends to 250°C, to 110°C, or is restricted to 25°C. It is based on many sources (see BSC, 2007b), but draws in particular from the work of Pabalan and Pitzer (1987) and Greenberg and Møller (1989). The YMP databases have some regulatory cachet as qualified products of what was an NQA-1 program.

The purpose of the present task is to improve these databases for use on the Used Fuel Disposition Campaign, doing so in an orderly and transparent way that will support qualification in support of the future underground high level nuclear waste disposal. The intent is that the UFDC work will utilize the same conventions and methodologies for treating thermodynamic data, unless substantive reasons drive a change. The Yucca Mountain Project was based on disposal in volcanic stuff, in a thick vadose zone in which oxidizing conditions were expected to prevail. A 50 year period of tunnel ventilation was planned to limit maximum temperature. Concentrated solutions were not originally expected at Yucca Mountain. Later concerns about dust deliquescence and evaporative concentration led to the development of the YMP concentrated solutions thermodynamic database (see BSC, 2007b). The Yucca Mountain design scenario was unique among those considered in repository research. Planned repositories in other countries have envisioned disposal below the water table (generally under reducing conditions) in clay, salt, granite or other hard rock, usually incorporating relatively low maximum temperature in the designs. The Used Fuel Disposition Campaign is investigating potential

disposal in mined repositories in these three rock types, plus a deep borehole option (which implies some kind of “hard” rock as the host rock). However, the UFDC may consider higher maximum temperatures than are presently being considered elsewhere.

Although the Yucca Mountain Project thermodynamic databases incorporated many data of value to generic geochemistry applications, in some areas the development was limited owing to the specific rock type, the expected oxidizing conditions, and limited maximum temperatures associated with the repository design. Consequently, these databases need additional development to adequately address the different design scenarios currently being studied by the UFDC. There is a need to address a wider range of minerals and aqueous species due to different rock types and expected reducing conditions. Finally, in any effort using thermodynamic data, there is the ever present factor of flaws being discovered in existing data, and the potential impact of newly reported data. Errors (and the suspicion of errors) often come to light in the application of the data. Activities impacting thermodynamic data are occurring in geochemistry and related fields on a continuing basis.

National and international standards organizations largely left the field some time ago in regard to thermodynamic data pertinent to geochemistry applications. The last major work by NIST (then NBS) was the volume published by Wagman et al. (1982), followed by an errata to the same (Wagman et al., 1989). CODATA published its last key thermodynamics report (Cox et al., 1989) in the same time period. The NEA thermodynamic data volumes (starting with Grenthe et al., 1992, and continuing to the present day) seem to represent the closest thing to a sanctioned body of work that is still active. However, the NEA has focused mainly on radionuclide elements, which is helpful but not complete for geochemistry applications in radioactive waste disposal.

The present report details progress in a current effort to develop thermodynamic data and models for complex clay minerals, with some attention on related sheet silicates (principally illites, celadonites, and chlorites), building on and updating data and models that were developed for the YMP database, using linear free energy and similar estimation methods discussed in detail by BSC (2007a). The previous effort on clays was limited due to the low importance of these minerals in the Yucca Mountain repository design (the host rock contained little clay, particularly in the near-field environment, and there was no planned use of engineered clay). The major shortcoming of the previous work from a UFDC perspective is that it followed some previous development (Tardy and Garrels, 1974; Wolery, 1978) in which the hydration state of smectite clays is treated implicitly. The effects of hydration/dehydration on properties such as molar volumes (and the consequent development of swelling pressure in a confined system) are ignored. There are some other deficiencies having to do with assumptions used in extrapolating the model properties (particularly cation exchange) to elevated temperature.

This effort is part of a larger one being conducted by in collaboration with Carlos Jove-Colon of SNL. This report presents updated and new baseline data for the sheet silicates of interest. In particular, data are presented for dehydrated smectites and some hydrated equivalents. Apart from the hydrated smectites, the data presented cover Gibbs energies and enthalpies of formation, entropies, and molar volumes (all for a 298.15K and 1 bar pressure) and Maier-Kelley heat capacity coefficients. For the hydrated smectites, data are presented for all of these

quantities except Gibbs energies and enthalpies of formation. Those quantities will be addressed in future work by evaluating models and data for smectite hydration/dehydration ,and the data and models will be further tested by addressing data for ion exchange involving interlayer cations (a phenomenon that is deeply tied to hydration/dehydration). The hydrated smectite data that are developed here will be used in that analysis. The methods used in the work presented here are those that have been used previously (BSC, 2007a), except that the baseline regressions for Gibbs energies have been revised using a slightly different set of "silicated" oxide components and that for hydrated smectites, the hydration state is now explicitly treated (the actual maximum hydration state is slightly contentious and a subject of planned future work.

This report is an updated version of a previous report (*Thermodynamic Database Development, with Emphasis on Complex Clay Minerals*, Level 4 Milestone (M4): M41UF033201, July 29, 2011). That report discussed the clay mineral issues from a UFDC perspective, recognized that some of the YMP-generated thermodynamic data for implicitly hydrated smectites were more properly assigned to corresponding dehydrated compositions, and laid out elements to a path forward. The estimated thermodynamic data presented in the present report are new. Some additional information pertinent to the understanding of clay minerals is also new.

Clay Minerals: Background

Clay minerals play various roles in the geologic disposal of nuclear waste, potentially being present as both host rock minerals and EBS components. [for an overview of clays from the perspective of the UFD Natural Systems department, see Chapter 4 of *Natural System Evaluation and Tool Development – FY11 Progress Report*: Wang et al., 2011]. Clay minerals are nearly ubiquitous at some level in nearly all rock types, ranging from minor alteration components in igneous rocks to major components in sedimentary rocks, notably shales and claystones. Clays may be used as components (often with modification) in an engineered repository, usually in an attempt to limit the access of water to waste containers and/or waste forms. Clays may form (or transform, potentially to other clay or non-clay minerals) in a repository, in response to water circulation, associated chemical transport, and the thermal field that decaying waste may generate.

Clay minerals are sheet silicates that have a very wide range of chemical compositions and which exhibit complex behavior. Some clay and clay-like minerals, such as kaolinite ($Al_2Si_2O_5(OH)_4$) and pyrophyllite ($Al_2Si_4O_{10}(OH)2_)$ have a narrow range of chemical composition and relatively simple crystallographic structure. The more complex clays, including the illites, smectites, and vermiculites, vary considerably in chemical composition and are somewhat more complex structurally (in part due to the variable chemical composition). Complex clays (and in most instances, simple clays as well) have crystal sizes that are < 2 μm. Imaging generally requires methods like Scanning Electron Microscopy (Figure 1 shows an SEM image of smectite showing a common "wet cornflakes" appearance). Complex clay mineral crystals of 10 μm size would be considered "large"). Such small crystals correlate with high specific surface area. The small size also makes it difficult to separate natural samples from mixtures containing small grains of other minerals. Furthermore, chemical interactions may take place in different parts of a clay crystal, and at different rates. The interpretation of experimental

measurement of the thermodynamic properties of complex clays is difficult because the number of variables that can affect results is generally too high to permit full control.

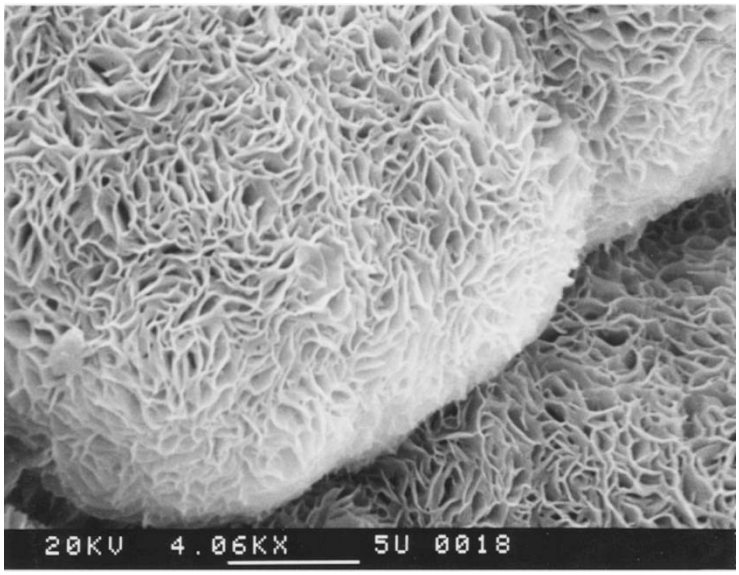

Figure 1. SEM image of smectite from Yucca Mountain Nevada (taken by Steve Chipera, Los Alamos National Laboratory).

Smectites are probably the most complex clays, as well as one of the most important types geologically. Smectites are a layered class of clay minerals that are comprised of repeating, parallel nanoscale sheets. Each framework sheet is composed of an octahedral layer of molecules that is sandwiched between two tetrahedral layers (forming a "t-o-t" structure; see Figure 2). Each tetrahedron is arranged so that a point joins the octahedral layer and a base is exposed on the outside of the t-o-t structure. The center of a tetrahedron in the t-layer is typically occupied by Si^{4+}, but Al^{3+} can substitute, leading to a net negative charge in the layer. Similar, the center of an octahedron in the o-layer is typically occupied by Al^{3+}, Mg^{2+}, Fe^{2+}, Fe^{3+}, and Li^{+}, and usually also by some vacancies. The o-layer can also develop electrical charge. Oxygen is located at the vertices of the tetrahedra and octahedra and some oxygens are shared by adjoining t- and o-layers. Minor hydrogen is tied to some oxygens.

In smectites, t-o-t sheets are separated by a layer (the *interlayer*) that contains mono- and divalent cations (e.g., Na^{+}, Ca^{2+}) and water. In a fully hydrated smectite, the interlayer is thought to contain two or more layers of water molecules. The exact state of maximum hydration is somewhat contentious. Ransom and Helgeson (1993) estimated it from basal spacing data to be 4.5 moles H_2O per "$O_{10}(OH)_2$" in the common molar formula of smectite (corresponding to ½ unit cell), where the "$(OH)_2$" is considered as containing *structural* water. Others tend to put it higher. For example, Liu and Lin (2005) evaluated different experimental data using the Ransom and Helgeson model framework and concluded that maximum hydration corresponded to 7.14 moles H_2O per "$O_{10}(OH)_2$" The maximum hydration number in these models is somewhat of a fictive construct, as the calculated hydration number for a smectite in equilibrium with liquid water (thermodynamic activity of water near unity) is generally something less. Ransom and Helgeson (1994b) calculate that homoionic (one exchangeable cation) smectites in contact with liquid water have actual hydration numbers that depend on the cation, and which depend strongly

on the cation charge (divalent cations have hydration numbers close to the maximum, monovalents have notably smaller ones). Cations in the interlayer are easily exchanged with aqueous solution and smectites in nature are not homoionic. Interlayer water can be removed by heating and other means, to the point that the interlayer becomes essentially dry.

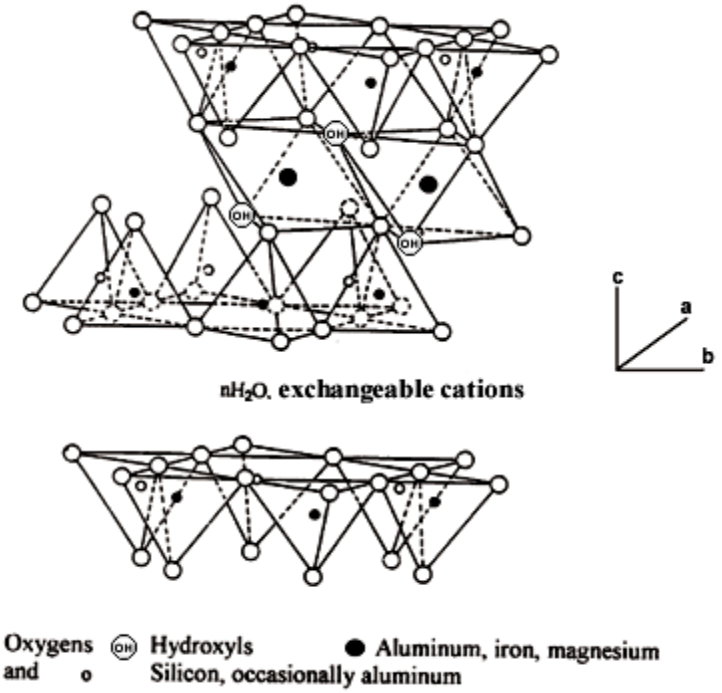

Figure 2. The crystal structure of smectite, showing a t-o-t framework layer at the top, with an interlayer shown below, with the t-layer of another t-o-t framework layer shown below that. Figure reproduced from Valenzuela Diaz and de Souza Santos (2001) under the terms of a Creative Commons Attribution License.

Smectites are generally divided into the following types:

- Beidellites, which are aluminous. The o-layer is mainly filled with Al^{3+} and vacancies in nearly 2:1 ration (little or no net electrical charge, and electrical charge is developed in the t-layer by substitution of Al^{3+} or Si^{4+}. The composition of an idealized sodium beidellite is $Na_{0.33}Al_2Al_{0.33}Si_{3.67}O_{10}(OH)_2$.
- Nontronites, which are ferric iron rich: Like beidellites, but with Fe^{3+} replacing Al^{3+} in the o-layer. The composition of an idealized sodium nontronite is $Na_{0.33}Fe_2Al_{0.33}Si_{3.67}O_{10}(OH)_2$.
- Saponites, which are magnesium rich: Like beidellites, but with Mg^{2+} replacing Al^{3+} in the o-layer. The composition of an idealized sodium saponite is $Na_{0.33}Mg_3Al_{0.33}Si_{3.67}O_{10}(OH)_2$.
- Montmorillonites: Unlike the above types, electrical charge in the framework is developed in the o-layer, typically by the substitution of some Mg^{2+} for Al^{3+}, while the t-layer is remains largely uncharged. The composition of an idealized sodium montmorillonite is $Na_{0.33}Mg_{0.33}Al_{1.67}Si_4O_{10}(OH)_2$.

- Hectorites (rare), which are lithium rich: Like montmorillonites, but with Mg^{2+} and Li^{+} in the o-layer.

Ion exchange in smectites (and vermiculites, which are like smectites but have higher framework charge and higher cation exchange capacity) is rapid. However, ion exchange (and other sorptive processes) may occur not only in the interlayer, but also on the crystal edges and on the basal planes at the top and bottom of the crystal. One would like to distinguish the effects at these different loci. However, it is difficult to do so, and often the gross effect is represented by a lumped exchange constant or a distribution coefficient (K_d). Furthermore, while interactions in the interlayer and the outer clay crystal surface are relatively rapid (seconds to minutes), other reactions such as exchange of cations in the framework layer (o-layer or t-layer) and dissolution and growth of the framework layer itself probably occur much more slowly under most shallow crustal conditions owing to the need to break (or make) covalent bonds.

Illites can be thought of as similar to the smectites as they also have t-o-t framework layers. However, the "interlayers" have little or no water, and somewhat characteristically contain potassium ions, which tend not to easily exchange with aqueous solution. The ion exchange capacity is therefore relatively low. In general, due to common geologic occurrence in deep sedimentary basins and in geothermal systems, illites are often thought of as clays that form at higher temperatures than the smectites. However, dehydrated smectites are stable to very high temperatures as shown by dehydration experiments and experimental synthesis (to 1500°C in one study reported by Tamura et al., 2000). Other clay-like minerals such as pyrophyllite ($Al_2Si_4O_{10}(OH)_2$) and talc ($Mg_3Si_4O_{10}(OH)_2$) contain t-o-t frameworks that are electrically neutral overall and in each type of sublayer (thus no additional cations are required). These may be considered structural analogs, to a point, of smectites and illites.

One feature about the clays and related sheet silicates is that interlayer water (which is significant only in smectites and vermiculites, which have higher framework charge) appears to require a framework charge that falls in a certain range. On the zero-charge end are pyrophyllite and talc. These lack significant interlayer water (and interlayer cations). On the unit-charge end are the micas muscovite ($KAl_2AlSi_3O_{10}(OH)_2$) and paragonite ($NaAl_2AlSi_3O_{10}(OH)_2$). These also have effectively dry interlayers. In between, closer to the low end, are the smectites, with a charge number of about 0.33 (e.g., Na-beidellite, $Na_{0.33}Al_2Al_{0.33}Si_{3.67}O_{10}(OH)_2$). These do have interlayer water. Also containing interlayer water are the vermiculites, with a charge number of about 0.66 (e.g., Na-Vermiculite, $Na_{0.66}Al_2Al_{0.66}Si_{3.66}O_{10}(OH)_2$).

Interlayer cations are believed to be located mostly at specific sites that are related to the positions of hexagonal rings of tetrahedra in the t-layers. For any of the above sheet silicate types, there is one ring pair (one ring above the interlayer, another below) per $O_{10}(OH)_2$ (cf. Deer et al., 1962, chapters on muscovite and pyrophyllite). In muscovite and paragonite, these interlayer cation sites are completely filled. Presumably there is insufficient room for interlayer water, or the geometric layout of interlayer cations and negatively oxygens from the facing side of the t-layers is unfavorable for the addition of water molecules. The interlayer cations likely act as pillars to separate the framework layers on each side. However, they may act to hold them tightly in place as well. In pyrophyllite and talc, the interlayer cation sites are all empty, and the absence of water is presumably due to lack of cations to attract the negatively charged oxygens

of water molecules and/or insufficient space (in the absence of interlayer cations acting as pillars to support the interlayer). For the case of only monovalent interlayer cations, about one in three interlayer cation sites are filled in smectites, about two in three in vermiculites. For the case of only divalent interlayer cations, these conditions change to one in six and one in three. Presumably such interlayer cations occupancies offer favorable combinations of attraction of water to the cations, sufficient space, and possibly also favorable configurations in regard to interactions between the hydrogen atoms of water and the interlayer-facing oxygen atoms of the t-layers. This is an area where a better understanding might be obtained, for example from molecular dynamics calculations.

Clay Minerals: Thermodynamic Data

Thermodynamic data and models for the complex clays (including the all-important smectites and illites) have always been problematic to geochemists. Typical experimental approaches such as solubility and calorimetry have been of limited value owing to the reactive nature of these phases and the difficulty in adequately characterizing them. Thus, models are generally used to estimate the relevant thermodynamic data from corresponding data for related phases, generally including simple clays, clay-like minerals, and other sheet silicates including various micas and chlorites.

One of the best known of these is the model of Tardy and Garrels (1974), which derives data for the Gibbs energies of "silicated" oxide components from the known Gibbs energies of the related sheet silicates (kaolinite, micas, chlorites). The Gibbs energies of these "silicated" oxides are generally different from those of the corresponding real oxides, and the difference is referred to as the free energy of silication. A correlation with cation electronegativities developed by Tardy and Garrels (1974) suggests that the free energies of silication of SiO_2 and Fe_2O_3 should be nearly zero and provides one means of extending the set of treatable oxides (whether the free energy of silication should be zero or not). Estimated values for other thermodynamic properties (entropies, heat capacities, and molar volumes) can be estimated by a variety of similar "additive" or quasi-additive schemes (cf. Helgeson et al., 1978; Ransom and Helgeson, 1994a), though methods for obtaining entropies and heat capacities usually use the properties of real oxides. These additional properties are needed to extrapolate the Gibbs energy with respect to temperature (entropy, heat capacity) and pressure (volume).

Tardy and Garrels (1974) developed a similar set of data for oxide components s corresponding to exchangeable cations (e.g., $Na_2O_{(ex)}$). These data are derived from ion exchange constant data. The assumption is made (see Tardy and Garrels, 1974) that the free energy of $K_2O_{(ex)}$ is the same as that for silicated K_2O. Although Tardy and Garrels (1974) offer a justification for this, it is not entirely compelling. The development of data for these exchangeable oxide components allows the method to be applied to clays with exchangeable interlayer cations, which are likely to behave distinctly from the corresponding non-exchangeable interlayer cations such as K_2O in muscovite (or so Tardy and Garrels thought). Tardy and Garrels argued that using a second set of oxide components for interlayer cations was justified because a different set of values could be obtained from the data at hand. Using the data for exchangeable components to calculate Gibbs energies for end-member components forces a simple mixing model to be consistent with the original ion exchange data.

However, when Tardy and Garrels developed their model, they did not explicitly account for the water in the interlayer. Therefore, results from there procedure for say an idealized Na-beidellite of formula $Na_{0.33}Al_2Al_{0.33}Si_{3.67}O_{10}(OH)_2$ would imply the interlayer water through the usage of the exchangeable oxide $Na_2O_{(ex)}$. However, this sort of treatment is not suficient if the loss or gain of interlayer water is sufficient to affect other clay properties of interest (e.g., swelling pressure) or change the local mass balance, for example by diluting or concentrating contacting aqueous solution.

As noted previously, Ransom and Helgeson (1993) calculated that a fully hydrated smectite would have about 4.5 H_2O of interlayer water per $O_{10}(OH)_2$ in the chemical formula, equivalent to about 2 water layers in the interlayer. Liu and Lin (2005) using the framework of the Ransom and Helgeson model to interpret a different set of hydration/dehydation data (Fu et al., 1990). They calculated 7.14 H_2O of interlayer water per formula unit for a fully hydrated smectite.

Another factor is that if one were to extrapolate the stabilities of the exchangeable oxide components to higher temperature and pressure, one should be using corresponding entropy, heat capacity, and molar volume functions also derived from exchange data. In fact, exchange data at elevated temperatures and pressures are difficult to come by. We have conducted a literature search for such data and will be using it in future analysis. We may also in the future conduct related experimental work.

In the Ransom and Helgeson hydration/dehydration model, the actual maximum hydration number (corresponding to unit water activity) in these models is generally less than the model maximum (notably so for monovalent interlayer cations, somewhat so for divalents). The model approach is to consider hydration/dehydration in the context of a regular solution mixing model, in which the end members are a dehydrated or anhydrous form ("as") and a maximally hydrated form ("hs"), for which the hydration number may be somewhat arbitrary. When the models are fit to data for relative humidity (equivalent to activity of liquid water) as a function of the mole fraction for of the fully hydrated component (x_{hs}), two parameters are obtained: log K for the reaction hs = as + nH_2O, where n is the maximal hydration number, and W_s, which is the Margules parameter (non-ideality parameter) for the regular solution model. The actual equations are somewhat complex and will not be presented here. At this time, we will merely note some key results.

When evaluated for unit water activity (see Ransom and Helgeson, 1993b), smectite compositions have actual hydration numbers less than the model maximum value (more so for monovalent interlayer ions than divalents). Thus, part of the hydrous end of the model may not be expressed under real conditions. These models suggest that when hydrating a fully dehydrated smectite, the Gibbs energy of the first-added H_2O has one value, the second someting different, and so forth, with the Gibbs energy of later-added H_2O approaching that of pure liquid water. Thus, to accurately model hydration/dehydration, the interlayer H_2O component cannot be treated in a linear fashion. However, properties other than the Gibbs energy and enthalpy can be estimated for hydrated smectites using linear and quasi-linear methods (cf. Ransom and Helgeson, 1994a).

An interlayer cation is the same physical species, whether it is formally treated using an "exchangeable" oxide component with implicit water or a silicated oxide component with explicit water. When a sodium smectite dissolves, the reaction can be written as producing either aqueous Na^+ ion from $Na_2O_{(ex)}$ (using the implicitly hydrated smectite formula) or aqueous Na^+ plus liquid H_2O (using the explicit smectite hydration number pertinent to the case for unit water activity). The results of the two model approaches must be consistent. This provides a way of reconciling the models for implicitly and explicitly hydrated smectites. A better test, however, would be to compare results for cation exchange reactions using implicitly and explicitly hydrated components, as this avoids the assumption (originally proposed by Tardy and Garrels, 1974) that the Gibbs energies for "exchangeable" and "silicated" K_2O components are equal.

Using schemes like the Tardy and Garrels (1974) estimation method, one can calculate the properties of a clay mineral or other sheet silicate by stoichiometrically summing the values for the relevant oxides. For greater accuracy, such estimations may be made by using component oxide substitutions starting with a closely related phase for which real data exist, such as pyrophyllite ($Al_2Si_4O_{10}(OH)_2$). [The late Robert M. Garrels used say, "Pyrophyllite is the mother of montmorillonite" to make this point.] Another factor may be to explicitly account for mixing effects, using the basic estimation methods to define the properties of end-members, and assuming (usually) ideal mixing in the site-mixing sense to define the properties of phases of intermediate composition.

The last YMP dilute systems thermodynamic database (data0.ymp.R5) contains data derived by such means for some clay compositions shown below in Table 1. A detailed description of the methods and derivation of the corresponding thermodynamic data is given in the Analysis/Model Report ANL-WIS-GS-000003 Rev. 1 (BSC, 2007a). Basically, this development follows Wolery (1978), who applied the Tardy-Garrels method but using updated values for the Gibbs energy data used to regress the values for the silicate oxides and also, in the case of subsequent calculation of equilibrium constants, updated values for the Gibbs energies of the relevant aqueous species. The later YMP work applied another level of updating. Data were obtained for five idealized beidellites, five idealized montmorillonites, five idealized saponites, five idealized nontronites, three complex smectites, an illite, and three idealized celadonites. Some data were also obtained by the same process for some chlorite and chlorite-related sheet silicates.

The previous estimation exercise has been revised and extended in a number of ways. The most significant is that explicitly dehydrated and hydrated smectite compositions are now treated, in addition to the implicitly hydrated smectite compositions addressed previously. For explicitly hydrated smectite compositions, various plausible maximum values of the interlayer hydration number were used. Calculations for estimating Gibbs energies and molar volumes are now done using a modified, consistent set of silicated oxide components. This set of silicated oxide components was also used to generate a set of alternative values for molar enthalpies, although these values were only used as a check on adopted values calculated from the Gibbs energies and molar enthalpies of the target minerals. The adopted enthalpy values satisfy the consistency relationship $\Delta G^\circ_f = \Delta H^\circ_f - \Delta S^\circ_f$, where ΔS°_f is calculated from the entropy of the target mineral and the entropies of the elements in their reference forms. Enthalpies were not included in the previous exercise (BSC, 2007a). The remaining thermodynamic properties were calculated using

the same methods used in that exercise. All calculations presented or discussed below were carried out in the spreadsheet Clays_TJW_2_Rev1.xlsx.

The new calculations follow the previous ones (e.g., BSC, 2007a) in using obsolete calorie units. This is partly for continuity, and partly to avoid introducing potential numerical inconsistencies at intermediate steps. The final results can be converted to joule units if desired, noting that 1 calorie = 4.184 joule.

Table 1 shows the compositional matrix used in the present work for estimating Gibbs energies. A previously employed $Mg(OH)_2$ component was dropped in favor of just using MgO and H_2O (structural water). The single Al_2O_3 component used in the Yucca Mountain work was replaced by octahedral and tetrahedral forms used in the earlier work by Wolery (1978). As noted previously, the same set of components was also used to estimate molar volumes and to make alternative estimates of molar enthalpies.

In the above derivations, the actual amount of water in the exchange layer of a smectite (beidellite, montmorillonite, saponite, nontronite, or "smectite") was not explicitly taken into account (this water does not include the water that is structurally bound in the $(OH)_2$ part of the formula). . In deriving the data for the Na-beidellite, for example, the exchangeable sodium was represented by the $Na_2O_{(ex)}$ component. The associated water can be thought of as being dealt with implicitly, as noted previously. Interestingly, using the silicated Na_2O component instead would yield data for the dehydrated equivalent of this hydrated clay, which is something that we intend to do in future development. We note that data for exchangeable oxide components was based only on 25°C data, and that the temperature dependence of the properties of the exchangeable components was assumed to be the same as those of the corresponding non-exchangeable components. This reduces the reliability of the estimated data at elevated temperature (in particular, the stabilities of affected clays with respect to other minerals becomes more uncertain). Also, because the water in the exchange layer is treated implicitly, dehydration cannot be properly accounted for.

Tables 2 and 3 show the results of the Gibbs energy regression, using known data for the sheet silicate minerals shown. Mathematically, the problem is a linear regression. The objective is to fit oxide component properties to known data for a set of minerals. Excel's regression tool is used for this purpose. Tables 4- 6 are analogous to Tables 1-3 and show the corresponding results for molar volumes. Analogous results for alternate values for enthalpies obtained using the same composition matrix as for Gibbs energies are not included in this report, but can be found in the spreadsheet for all the new estimates presented or discussed in this report (Clays_TJW_2_Rev1.xlsx). Table 7 shows values for interlayer water properties from Ransom and Helgeson (1994b). Here data are missing for the Gibbs energy and enthalpy, as those must be evaluated from models that are not linear in the interlayer water component, as noted previously. Dealing with that will be the focus of future work, as noted previously. However, it is noted that the spreadsheet facilitates calculations with any such data one might wish to experiment with.

Table 8 shows the reference reactions that were used to estimate the Gibbs energies (and molar volumes) of chlorites and related minerals, an illite, and some celadonites (which are related to

illite). The corresponding Gibbs energy and molar volume estimates are given in Table 9, along with corresponding estimates for enthalpy, entropy, and Maier-Kelly heat capacity coefficients. A slightly different set of reference reactions was to make estimates for entropies and heat capacity coefficients. A key difference is the use of a single Al_2O_3 component. For heat capacity coefficients, the oxide component values correspond to the actual oxides. This is also true in the case of entropies, although the actual computation is non-linear, but has linear parts (Helgeson et al., 1978, eq 75, p. 51: $S° = \Delta S_s°*(\Delta V_s° + V°)/(2*\Delta V_s°) - 2$(cal/mol-K)*(# of ferrous Fe's per mole)). Here $\Delta S_s°$ is computed from a reference reaction involving actual oxide components, and could itself be taken as an estimate of S°, albeit a less accurate one. $\Delta V_s°$ is an analogous result for volumes. V° is the molar volume, which in many cases must also be an estimate.

Table 10 shows the reference reactions that were used to estimate the Gibbs energies (and molar volumes) of 23 dehydrated smectite compositions. The corresponding Gibbs energy and molar volume estimates are given in Table 11, along with corresponding estimates for enthalpy, entropy, and Maier-Kelly heat capacity coefficients. Again, slightly different set of reference reactions was to make estimates for entropies and heat capacity coefficients. Tables 12, 13, and 14 present estimated thermodynamic properties (without values for Gibbs energies and enthalpies, due to the reasons noted previously) for the corresponding hydrated smectites with hydration numbers of 4.5, 5, and 7, respectively. These data will be used in evaluating hydration/dehydration models to complete a model treating smectite hydration.

Table 15 shows revised Gibbs energy estimates only, for the corresponding implicitly hydrated smectite compositions. Previous estimates of the remaining thermodynamic properties (e.g., Wolery, 1978; BSC, 2007a) were not based on cation exchange data, and, as noted previously, would have been more properly applied to fully dehydrated smectite.

Table 16 shows a compilation of values for the entropies of the elements in their reference forms and identifies the values adopted for the present study. This list includes only data for elements that are needed for work on clay minerals and related sheet silicates, for the present work and the foreseeable future. For the most part, the adopted values are taken from the NEA thermodynamic data series (e.g., Grenthe et al., 1992 and succeeding volumes). NEA generally adopts CODATA (Cox et al., 1989) data, as much as possible. No source examined appears to cover all of the chemical elements.

The data calculated here provides the basis for ongoing work to evaluate models for explicitly hydrated smectites, and should be sufficient for that purpose. However, it is noted that revisions may be made to these results due to future revisions in the thermodynamic data used as input. For example, we are now considering such revisions in regard to the Gibbs energies of kaolinite and pyrophyllite. The spreadsheet (Clays_TJW_2_Rev1.xlsx) is easily revisable should such input data be revised. Also, the spreadsheet is supportive of easy calculation of the properties of any of the explicitly hydrated smectites if results are desired for hydration numbers other than those now used in it.

Table 1. Composition Matrix for Regressing Gibbs Energies of Silicated Oxides from the Known Gibbs Energies of Some Sheet Silicate Minerals. The samecomposition matrix was used to estimate alternate values of enthalpies, which are not presented in thisreport. In the regressions, the data for Antigorite were scaled by a factor of 1/12 to avoid a much higher effective weighting for this mineral, which has a very large molecular formula. Quartz and Hematite are included in the regression, even though they are not sheet silicates. A justification for this is given by Wolery (1978) and BSC (2007a).

Name	**Formula**	K2O	Na2O	CaO	MgO	Fe2O3	FeO	Al2O3(oct)	Al2O3(tetr)	SiO2	H2O
14A-Clinochlore	Mg5AlAlSi3O10(OH)8	0	0	0	5	0	0	0.5	0.5	3	4
7A-Clinochlore	Mg5AlAlSi3O10(OH)8	0	0	0	5	0	0	0.5	0.5	3	4
Annite	KFe3AlSi3O10(OH)2	0.5	0	0	0	0	3	0	0.5	3	1
Antigorite	Mg48Si34O85(OH)62	0	0	0	4	0	0	0	0	2.83333	2.58333
Chrysotile	Mg3Si2O5(OH)4	0	0	0	3	0	0	0	0	2	2
Hematite	Fe2O3	0	0	0	0	1	0	0	0	0	0
Kaolinite	Al2Si2O5(OH)4	0	0	0	0	0	0	1	0	2	2
Margarite	CaAl2Al2Si2O10(OH)2	0	0	1	0	0	0	1	1	2	1
Muscovite	KAl2AlSi3O10(OH)2	0.5	0	0	0	0	0	1	0.5	3	1
Paragonite	NaAl2AlSi3O10(OH)2	0	0.5	0	0	0	0	1	0.5	3	1
Phlogopite	KMg3AlSi3O10(OH)2	0.5	0	0	3	0	0	0	0.5	3	1
Pyrophyllite	Al2Si4O10(OH)2	0	0	0	0	0	0	1	0	4	1
Quartz	SiO2	0	0	0	0	0	0	0	0	1	0
Talc	Mg3Si4O10(OH)2	0	0	0	3	0	0	0	0	4	1

Table 2. Fitting error in the Gibbs energy regression for silicate minerals.

Name	**Formula**	ΔG_f^o cal/mol	Calculated ΔG_f^o cal/mol	Error cal/mol	% Error
14A-Clinochlore	Mg5AlAlSi3O10(OH)8	-1961703	-1959402.0	2301.0	-0.1173
7A-Clinochlore	Mg5AlAlSi3O10(OH)8	-1957101	-1959402.0	-2301.0	0.1176
Annite	KFe3AlSi3O10(OH)2	-1147156	-1147156.0	0.0	0.0000
Antigorite	Mg48Si34O85(OH)62	-1317335	-1317238.9	96.1	-0.0073
Chrysotile	Mg3Si2O5(OH)4	-964871	-965879.6	-1008.6	0.1045
Hematite	Fe2O3	-178155	-178155.0	0.0	0.0000
Kaolinite	Al2Si2O5(OH)4	-905614	-904725.5	888.5	-0.0981
Margarite	CaAl2Al2Si2O10(OH)2	-1394150	-1394150.0	0.0	0.0000
Muscovite	KAl2AlSi3O10(OH)2	-1336301	-1335667.0	634.0	-0.0474
Paragonite	NaAl2AlSi3O10(OH)2	-1326012	-1326012.0	0.0	0.0000
Phlogopite	KMg3AlSi3O10(OH)2	-1396187	-1396821.0	-634.0	0.0454
Pyrophyllite	Al2Si4O10(OH)2	-1255997	-1257519.5	-1522.5	0.1212
Quartz	SiO2	-204656	-204656.0	0.0	0.0000
Talc	Mg3Si4O10(OH)2	-1320188	-1318673.5	1514.5	-0.1147

Table 3. Gibbs energies of silicated oxides, obtained from the Gibbs energy regression.

Oxide	Silicated ΔG_f^o cal/mol	Unsilicated ΔG_f^o cal/mol	Silication ΔG_f^o cal/mol
K2O	-187699.1	-77056.0	-110643.1
Na2O	-168389.1	-89883.0	-78506.1
CaO	-168034.6	-144366.0	-23668.6
MgO	-147843.8	-136086.0	-11757.8
Fe2O3	-178155.0	-178155.0	0.0
FeO	-64622.2	-60097.0	-4525.2
Al2O3(oct)	-382377.4	-374824.0	-7553.4
Al2O3(tet)	-377907.9	-374824.0	-3083.9
SiO2	-204656.0	-204656.0	0.0
H2O	-56518.0	-----	-----

Table 4. Composition Matrix for Regressing Molar Volumes of Silicated Oxides from the Known Volumes of Some Sheet Silicate Minerals. This composition matrix is similar to that used to regress Gibbs energies (Table 1). However, a larger number of minerals are included in the present case, reflecting a greater availability of mineral volume data. Again, the data for Antigorite were scaled by a factor of 1/12 to avoid a much higher effective weighting for this mineral, which has a very large molecular formula. Quartz and Hematite are again included in the regression, even though they are not sheet silicates.

Name	**Formula**	K2O	Na2O	CaO	MgO	Fe2O3	FeO	Al2O3(oct)	Al2O3(tetr)	SiO2	H2O
14A-Amesite	Mg4Al2Al2Si2O10(OH)8	0	0	0	4	0	0	1	1	2	4
14A-Clinochlore	Mg5AlAlSi3O10(OH)8	0	0	0	5	0	0	0.5	0.5	3	4
14A-Daphnite	Fe5AlAlSi3O10(OH)8	0	0	0	0	0	5	0.5	0.5	3	4
7A-Amesite	Mg2AlAlSiO5(OH)4	0	0	0	2	0	0	0.5	0.5	1	2
7A-Chamosite	Fe2AlAlSiO5(OH)4	0	0	0	0	0	2	0.5	0.5	1	2
7A-Clinochlore	Mg5AlAlSi3O10(OH)8	0	0	0	5	0	0	0.5	0.5	3	4
7A-Cronstedtite	Fe2FeFeSiO5(OH)4	0	0	0	0	1	2	0	0	1	2
7A-Daphnite	Fe5AlAlSi3O10(OH)8	0	0	0	0	0	5	0.5	0.5	3	4
Annite	KFe3AlSi3O10(OH)2	0.5	0	0	0	0	3	0	0.5	3	1
Antigorite	Mg48Si34O85(OH)62	0	0	0	4	0	0	0	0	2.83333	2.58333
Celadonite	KMgAlSi4O10(OH)2	0.5	0	0	1	0	0	0.5	0	4	1
Chrysotile	Mg3Si2O5(OH)4	0	0	0	3	0	0	0	0	2	2
Greenalite	Fe3Si2O5(OH)4	0	0	0	0	0	3	0	0	2	2
Hematite	Fe2O3	0	0	0	0	1	0	0	0	0	0
Kaolinite	Al2Si2O5(OH)4	0	0	0	0	0	0	1	0	2	2
Margarite	CaAl2Al2Si2O10(OH)2	0	0	1	0	0	0	1	1	2	1
Minnesotaite	Fe3Si4O10(OH)2	0	0	0	0	0	3	0	0	4	1
Muscovite	KAl2AlSi3O10(OH)2	0.5	0	0	0	0	0	1	0.5	3	1
Paragonite	NaAl2AlSi3O10(OH)2	0	0.5	0	0	0	0	1	0.5	3	1
Phlogopite	KMg3AlSi3O10(OH)2	0.5	0	0	3	0	0	0	0.5	3	1
Pyrophyllite	Al2Si4O10(OH)2	0	0	0	0	0	0	1	0	4	1
Quartz	SiO2	0	0	0	0	0	0	0	0	1	0
Sepiolite	Mg4Si6O15(OH)2:6H2O	0	0	0	4	0	0	0	0	6	7
Talc	Mg3Si4O10(OH)2	0	0	0	3	0	0	0	0	4	1

Table 5. Fitting error in the molar volume regression for silicate minerals.

Name	Formula	V^o cm^3/mol	Calculated V^o cm^3/mol	Error cm^3/mol	% Error
14A-Amesite	Mg4Al2Al2Si2O10(OH)8	205.400	202.053	-3.347	-1.6297
14A-Clinochlore	Mg5AlAlSi3O10(OH)8	207.110	209.857	2.747	1.3265
14A-Daphnite	Fe5AlAlSi3O10(OH)8	213.420	218.761	5.341	2.5025
7A-Amesite	Mg2AlAlSiO5(OH)4	103.000	101.026	-1.974	-1.9162
7A-Chamosite	Fe2AlAlSiO5(OH)4	106.200	104.588	-1.612	-1.5181
7A-Clinochlore	Mg5AlAlSi3O10(OH)8	211.500	209.857	-1.643	-0.7767
7A-Cronstedtite	Fe2FeFeSiO5(OH)4	110.900	110.076	-0.824	-0.7432
7A-Daphnite	Fe5AlAlSi3O10(OH)8	221.200	218.761	-2.439	-1.1027
Annite	KFe3AlSi3O10(OH)2	154.320	156.643	2.323	1.5050
Antigorite	Mg48Si34O85(OH)62	145.761	147.523	1.762	1.2089
Celadonite	KMgAlSi4O10(OH)2	157.100	150.826	-6.274	-3.9937
Chrysotile	Mg3Si2O5(OH)4	108.500	108.831	0.331	0.3051
Greenalite	Fe3Si2O5(OH)4	115.000	114.173	-0.827	-0.7190
Hematite	Fe2O3	30.274	31.098	0.824	2.7227
Kaolinite	Al2Si2O5(OH)4	99.520	100.552	1.032	1.0367
Margarite	CaAl2Al2Si2O10(OH)2	129.400	129.400	0.000	0.0000
Minnesotaite	Fe3Si4O10(OH)2	147.860	143.153	-4.707	-3.1837
Muscovite	KAl2AlSi3O10(OH)2	140.710	143.021	2.311	1.6425
Paragonite	NaAl2AlSi3O10(OH)2	132.530	132.530	0.000	0.0000
Phlogopite	KMg3AlSi3O10(OH)2	149.660	151.300	1.640	1.0961
Pyrophyllite	Al2Si4O10(OH)2	126.600	129.531	2.931	2.3153
Quartz	SiO2	22.688	22.182	-0.506	-2.2316
Sepiolite	Mg4Si6O15(OH)2:6H2O	285.600	285.711	0.111	0.0388
Talc	Mg3Si4O10(OH)2	136.250	137.810	1.560	1.1453

Table 6. Molar volumes of silicated oxides, obtained from the molar volumes regression.

Oxide	Silicated V^o cm^3/mol	Unsilicated V^o cm^3/mol	Silication ΔV^o cm^3/mol
K2O	45.543	40.380	5.163
Na2O	24.561	25.000	-0.439
CaO	18.432	16.764	1.668
MgO	11.233	24.630	-13.397
Fe2O3	31.098	11.248	19.850
FeO	13.014	30.274	-17.260
Al2O3(oct)	25.420	12.000	13.420
Al2O3(tet)	25.800	25.575	0.225
SiO2	22.182	22.688	-0.506
H2O	15.384	-----	-----

Table 7. Thermodynamic properties of interlayer water in smectite (Ransom and Helgeson, 1994b, Table 2, p. 4541.

$\Delta G_f°$	$\Delta H_f°$	S°	Cp°	a	b x 10^3	c x 10^{-5}	V°
kcal/mol	kcal/mol	cal/mol-K	cal/mol-K	cal/mol-K	cal/mol-K²	cal-K/mol	cm³/mol
-----	-----	13.15	11.46	9.044	12.34	-0.979	17.22

Table 8. Reference Reactions for Estimating Gibbs energies, molar volumes, and alternative enthalpy values for Chlorites and Related Minerals, an Illite, and Some Celadonites. The reference reactions used to estimate entropies and heat capacity coefficients are similar but slightly different (in particular, there is no distinction between octahedral and tetrahedral Al_2O_3).

Name	**Formula**	**Reference Reaction**
7A-Ripidolite	Mg3Fe2AlAlSi3O10(OH)8	7A-Ripidolite = 7A-Clinochlore + 2FeO - 2MgO
14A-Ripidolite	Mg3Fe2AlAlSi3O10(OH)8	14A-Ripidolite = 14A-Clinochlore + 2FeO - 2MgO
7A-Daphnite	Fe5AlAlSi3O10(OH)8	7A-Daphnite = 7A-Clinochlore + 5FeO - 5MgO
14A-Daphnite	Fe5AlAlSi3O10(OH)8	14A-Daphnite = 14A-Clinochlore + 5FeO - 5MgO
7A-Amesite	Mg2AlAlSiO5(OH)4	7A-Amesite = 7A-Clinochlore - 3MgO - 2SiO2 - 2H2O
14A-Amesite	Mg4Al2Al2Si2O10(OH)8	14A-Amesite = 14A-Clinochlore - MgO + 0.5Al2O3(oct) + 0.5Al2O3(tetr) - SiO2
7A-Chamosite	Fe2AlAlSiO5(OH)4	7A-Chamosite = 7A-Clinochlore- 5MgO + 2FeO - 2SiO2 - 2H2O
7A-Cronstedtite	Fe2FeFeSiO5(OH)4	7A-Cronstedtite = 7A-Clinochlore - 5MgO + 2FeO +Fe2O3 - 0.5Al2O3(oct) -0.5Al2O3(tetr) - 2SiO2 - 2H2O
Greenalite	Fe3Si2O5(OH)4	Greenalite = Chrysotile + 3FeO - 3MgO
Minnesotaite	Fe3Si4O10(OH)2	Minnesotaite = Talc + 3FeO - 3MgO
Illite	K0.6Mg0.25Al2.3Si3.5O10(OH)2	Illite = Pyrophyllite + 0.3K2O + 0.25MgO - 0.1Al2O3(oct) + 0.25Al2O3(tetr) - 0.5SiO2
Celadonite	KMgAlSi4O10(OH)2	Celadonite = Pyrophyllite + 0.5K2O + MgO - 0.5Al2O3(oct)
Ferroceladonite	KFeFeSi4O10(OH)2	Ferroceladonite = Pyrophyllite + 0.5K2O + 0.5Fe2O3 + FeO - Al2O3(oct)
Ferroaluminoceladonite	KFeAlSi4O10(OH)2	Ferroaluminoceladonite = Pyrophyllite + 0.5K2O + FeO - 0.5Al2O3(oct)

Table 9. Estimated Thermodynamic Data for Chlorites and Related Minerals, an Illite, and Some Celadonites. Data in purple cells are taken from Helgeson et al. (1978).

Name	Formula	$\Delta G_f°$ cal/mol	$\Delta H_f°$ cal/mol	S° cal/mol-K	V° cm^3/mol	a cal/mol-K	b x 10^3 cal/mol-K^2	c x 10^{-5} cal-K/mol
7A-Ripidolite	Mg3Fe2AlAlSi3O10(OH)8	-1792651.4	-1942787.4	126.147	215.380	166.700	51.280	39.420
14A-Ripidolite	Mg3Fe2AlAlSi3O10(OH)8	-1797253.4	-1946119.2	130.407	209.634	170.380	42.760	36.010
7A-Daphnite	Fe5AlAlSi3O10(OH)8	-1540992.6	-1686174.0	138.900	221.200	172.530	52.280	37.230
14A-Daphnite	Fe5AlAlSi3O10(OH)8	-1545594.6	-1689702.7	142.500	213.420	176.210	43.760	33.820
7A-Amesite	Mg2AlAlSiO5(OH)4	-991221.4	-1070157.5	52.000	103.000	81.030	24.738	20.230
14A-Amesite	Mg4Al2Al2Si2O10(OH)8	-1989345.9	-2145757.1	108.900	205.400	172.590	34.980	41.670
7A-Chamosite	Fe2AlAlSiO5(OH)4	-824778.1	-899159.5	64.700	106.200	84.910	25.400	18.770
7A-Cronstedtite	Fe2FeFeSiO5(OH)4	-622790.4	-694402.7	73.500	110.900	84.790	41.840	12.476
Greenalite	Fe3Si2O5(OH)4	-715206.0	-786483.0	72.600	115.000	81.650	32.600	15.390
Minnesotaite	Fe3Si4O10(OH)2	-1070523.0	-1153847.4	83.500	147.860	88.310	42.610	11.150
Illite	K0.6Mg0.25Al2.3Si3.5O10(OH)2	-1303178.9	-1394137.6	62.871	135.888	86.044	38.567	17.823
Celadonite	KMgAlSi4O10(OH)2	-1306501.6	-1395512.0	74.900	157.100	80.250	25.300	18.540
Ferroceladonite	KFeFeSi4O10(OH)2	-1121168.7	-1208082.5	80.400	152.514	85.062	52.089	11.867
Ferroaluminoceladonite	KFeAlSi4O10(OH)2	-1223280.0	-1311623.9	75.847	149.675	87.062	44.199	14.282

Table 10. Reference Reactions for Estimating Gibbs energies, molar volumes, and alternative enthalpy values for 23 Dehydrated Smectite Compositions. The reference reactions used to estimate entropies and heat capacity coefficients are similar but slightly different (in particular, there is no distinction between octahedral and tetrahedral Al_2O_3).

H-Beidellite	H0.33Al2.33Si3.67O10(OH)2	H-Beidellite = Pyrophyllite + 0.165H2O + 0.165Al2O3(tetr) - 0.33SiO2
Na-Beidellite	Na0.33Al2.33Si3.67O10(OH)2	Na-Beidellite = Pyrophyllite + 0.165Na2O + 0.165Al2O3(tetr) - 0.33SiO2
K-Beidellite	K0.33Al2.33Si3.67O10(OH)2	K-Beidellite = Pyrophyllite + 0.165K2O + 0.165Al2O3(tetr) - 0.33SiO2
Ca-Beidellite	Ca0.165Al2.33Si3.67O10(OH)2	Ca-Beidellite = Pyrophyllite + 0.165CaO + 0.165Al2O3(tetr) - 0.33SiO2
Mg-Beidellite	Mg0.165Al2.33Si3.67O10(OH)2	Mg-Beidellite = Pyrophyllite + 0.165MgO + 0.165Al2O3(tetr) - 0.33SiO2
H-Saponite	H0.33Mg3Al0.33Si3.67O10(OH)2	H-Saponite = Talc + 0.165H2O + 0.165Al2O3(tetr) - 0.33SiO2
Na-Saponite	Na0.33Mg3Al0.33Si3.67O10(OH)2	Na-Saponite = Talc + 0.165Na2O + 0.165Al2O3(tetr) - 0.33SiO2
K-Saponite	K0.33Mg3Al0.33Si3.67O10(OH)2	K-Saponite = Talc + 0.165K2O + 0.165Al2O3(tetr) - 0.33SiO2
Ca-Saponite	Ca0.165Mg3Al0.33Si3.67O10(OH)2	Ca-Saponite = Talc + 0.165CaO + 0.165Al2O3(tetr) - 0.33SiO2
Mg-Saponite	Mg0.165Mg3Al0.33Si3.67O10(OH)2	Mg-Saponite = Talc + 0.165MgO + 0.165Al2O3(tetr) - 0.33SiO2
H-Nontronite	H0.33Fe2Al0.33Si3.67O10(OH)2	H-Nontronite = Pyrophyllite + 0.165H2O + Fe2O3 - Al2O3(oct) + 0.165Al2O3(tetr) - 0.33SiO2
Na-Nontronite	Na0.33Fe2Al0.33Si3.67O10(OH)2	Na-Nontronite = Pyrophyllite + 0.165Na2O + Fe2O3 - Al2O3(oct) + 0.165Al2O3(tetr) - 0.33SiO2
K-Nontronite	K0.33Fe2Al0.33Si3.67O10(OH)2	K-Nontronite = Pyrophyllite + 0.165K2O + Fe2O3 - Al2O3(oct) + 0.165Al2O3(tetr) - 0.33SiO2
Ca-Nontronite	Ca0.165Fe2Al0.33Si3.67O10(OH)2	Ca-Nontronite = Pyrophyllite + 0.165CaO + Fe2O3 - Al2O3(oct) + 0.165Al2O3(tetr) - 0.33SiO2
Mg-Nontronite	Mg0.165Fe2Al0.33Si3.67O10(OH)2	Mg-Nontronite = Pyrophyllite + 0.165MgO + Fe2O3 - Al2O3(oct) + 0.165Al2O3(tetr) - 0.33SiO2
H-Montmorillonite	H0.33Mg0.33Al1.67Si4O10(OH)2	H-Montmorillonite = Pyrophyllite + 0.165H2O + 0.33MgO - 0.165Al2O3(oct)
Na-Montmorillonite	Na0.33Mg0.33Al1.67Si4O10(OH)2	Na-Montmorillonite = Pyrophyllite + 0.165Na2O + 0.33MgO - 0.165Al2O3(oct)
K-Montmorillonite	K0.33Mg0.33Al1.67Si4O10(OH)2	K-Montmorillonite = Pyrophyllite + 0.165K2O + 0.33MgO - 0.165Al2O3(oct)
Ca-Montmorillonite	Ca0.165Mg0.33Al1.67Si4O10(OH)2	Ca-Montmorillonite = Pyrophyllite + 0.165CaO + 0.33MgO - 0.165Al2O3(oct)
Mg-Montmorillonite	Mg0.495Al1.67Si4O10(OH)2	Mg-Montmorillonite = Pyrophyllite + 0.495MgO - 0.165Al2O3(oct)
Low Fe-Mg Smectite	see below	Low Fe-Mg Smectite = Pyrophyllite + 0.075Na2O + 0.1K2O + 0.02CaO + 0.9MgO + 0.08Fe2O3 + 0.29FeO - 0.5Al2O3(oct) + 0.125Al2O3(tetr) - 0.25SiO2
Fe-Mg Smectite	see below	High Fe-Mg Smectite = Pyrophyllite + 0.05Na2O + 0.1K2O + 0.025CaO + 1.15MgO + 0.1Fe2O3 + 0.5FeO - 0.625Al2O3(oct) + 0.125Al2O3(tetr) - 0.5SiO2
Reykjanes Smectite	see below	Reykjanes Smectite = Pyrophyllite + 0.165Na2O + 0.015K2O + 0.66CaO + 1.29MgO + 0.175Fe2O3 + 0.33FeO + 0.01MnO - 0.86Al2O3(oct) + 0.415Al2O3(tetr) - 0.83SiO2

Low Fe-Mg Smectite = Na0.15K0.2Ca0.02(Mg0.9Fe(+++)0.16Fe(++)0.29Al)(Al0.25Si3.75)O10(OH)2
Fe-Mg Smectite = Na0.1K0.2Ca0.025(Mg1.15Fe(+++)0.2Fe(++)0.5Al0.75)(Al0.5Si3.5)O10(OH)2
Reykjanes Smectite = Na0.33K0.03Ca0.66(Mg1.29Fe(+++)0.35Fe(++)0.33Mn0.01Al0.28)(Al0.83Si3.17)O10(OH)2

Table 11. Estimated Thermodynamic Data for 23 Dehydrated Smectite Compositions.

Name	Formula	$\Delta G_f°$ cal/mol	$\Delta H_f°$ cal/mol	S° cal/mol-K	V° cm^3/mol	a cal/mol-K	b x 10^3 cal/mol-K^2	c x 10^{-5} cal-K/mol
H-Beidellite	H0.33Al2Al0.33Si3.67O10(OH)2	-1260140.8	-1351137.7	57.636	126.075	81.438	38.333	17.774
Na-Beidellite	Na0.33Al2Al0.33Si3.67O10(OH)2	-1278599.5	-1368880.0	58.931	127.590	83.277	37.780	18.251
K-Beidellite	K0.33Al2Al0.33Si3.67O10(OH)2	-1281785.7	-1372093.1	59.896	131.052	83.319	38.401	17.919
Ca-Beidellite	Ca0.165Al2Al0.33Si3.67O10(OH)2	-1278541.0	-1368495.6	57.618	126.578	82.191	37.152	18.031
Mg-Beidellite	Mg0.165Al2Al0.33Si3.67O10(OH)2	-1275209.6	-1365228.7	57.050	125.391	81.945	37.260	18.018
H-Saponite	H0.33Mg3Al0.33Si3.67O10(OH)2	-1324331.8	-1409762.5	62.777	135.725	84.486	40.729	13.832
Na-Saponite	Na0.33Mg3Al0.33Si3.67O10(OH)2	-1342790.5	-1427505.2	64.071	137.240	86.325	40.176	14.309
K-Saponite	K0.33Mg3Al0.33Si3.67O10(OH)2	-1345976.7	-1430717.5	65.039	140.702	86.367	40.797	13.977
Ca-Saponite	Ca0.165Mg3Al0.33Si3.67O10(OH)2	-1342732.0	-1427120.5	62.760	136.228	85.239	39.548	14.089
Mg-Saponite	Mg0.165Mg3Al0.33Si3.67O10(OH)2	-1339400.6	-1423853.8	62.190	135.041	84.993	39.656	14.076
H-Nontronite	H0.33Fe2Al0.33Si3.67O10(OH)2	-1055918.4	-1140192.3	66.657	131.753	77.438	54.113	12.944
Na-Nontronite	Na0.33Fe2Al0.33Si3.67O10(OH)2	-1074377.1	-1157936.8	67.945	133.267	79.277	53.560	13.421
K-Nontronite	K0.33Fe2Al0.33Si3.67O10(OH)2	-1077563.2	-1161143.7	68.931	136.730	79.319	54.181	13.089
Ca-Nontronite	Ca0.165Fe2Al0.33Si3.67O10(OH)2	-1074318.6	-1157550.6	66.638	132.256	78.191	52.932	13.201
Mg-Nontronite	Mg0.165Fe2Al0.33Si3.67O10(OH)2	-1070987.1	-1154285.8	66.063	131.068	77.945	53.040	13.188
H-Montmorillonite	H0.33Mg0.33Al1.67Si4O10(OH)2	-1251018.7	-1340729.7	58.968	128.651	79.429	40.683	16.388
Na-Montmorillonite	Na0.33Mg0.33Al1.67Si4O10(OH)2	-1269477.4	-1358472.2	60.263	130.165	81.267	40.130	16.865
K-Montmorillonite	K0.33Mg0.33Al1.67Si4O10(OH)2	-1272663.5	-1361685.0	61.229	133.627	81.310	40.750	16.533
Ca-Montmorillonite	Ca0.165Mg0.33Al1.67Si4O10(OH)2	-1269418.9	-1358087.6	58.951	129.154	80.181	39.501	16.645
Mg-Montmorillonite	Mg0.495Al1.67Si4O10(OH)2	-1266087.4	-1354820.7	58.382	127.966	79.935	39.610	16.632
Low Fe-Mg Smectite	see below	-1261694.8	-1351295.0	65.313	134.706	84.327	41.014	15.634
High Fe-Mg Smectite	see below	-1213458.8	-1303302.8	66.390	131.625	86.685	40.089	15.493
Reykjanes Smectite	see below	-1299800.6	-1390109.9	69.942	138.295	90.231	39.005	15.618

Low Fe-Mg Smectite = Na0.15K0.2Ca0.02(Mg0.9Fe(+++)0.16Fe(++)0.29Al)(Al0.25Si3.75)O10(OH)2
Fe-Mg Smectite = Na0.1K0.2Ca0.025(Mg1.15Fe(+++)0.2Fe(++)0.5Al0.75)(Al0.5Si3.5)O10(OH)2
Reykjanes Smectite = Na0.33K0.03Ca0.66(Mg1.29Fe(+++)0.35Fe(++)0.33Mn0.01Al0.28)(Al0.83Si3.17)O10(OH)2

Table 12. Estimated Thermodynamic Data for 23 Smectite Compositions with interlayer hydration number of 4.5. The data in Table 4 for interlayer water properties are used along with the data for the corresponding dehydrated compositions from Table 8.

Name	Formula	$\Delta G_f°$ cal/mol	$\Delta H_f°$ cal/mol	S° cal/mol-K	V° cm^3/mol	a cal/mol-K	b x 10^3 cal/mol-K^2	c x 10^{-5} cal-K/mol
H-Beidellite	H0.33Al2Al0.33Si3.67O10(OH)2			116.811	203.565	122.136	93.863	13.368
Na-Beidellite	Na0.33Al2Al0.33Si3.67O10(OH)2			118.106	205.080	123.975	93.310	13.845
K-Beidellite	K0.33Al2Al0.33Si3.67O10(OH)2			119.071	208.542	124.017	93.931	13.513
Ca-Beidellite	Ca0.165Al2Al0.33Si3.67O10(OH)2			116.793	204.068	122.889	92.682	13.626
Mg-Beidellite	Mg0.165Al2Al0.33Si3.67O10(OH)2			116.225	202.881	122.643	92.790	13.612
H-Saponite	H0.33Mg3Al0.33Si3.67O10(OH)2			121.952	213.215	125.184	96.259	9.426
Na-Saponite	Na0.33Mg3Al0.33Si3.67O10(OH)2			123.246	214.730	127.023	95.706	9.903
K-Saponite	K0.33Mg3Al0.33Si3.67O10(OH)2			124.214	218.192	127.065	96.327	9.571
Ca-Saponite	Ca0.165Mg3Al0.33Si3.67O10(OH)2			121.935	213.718	125.937	95.078	9.684
Mg-Saponite	Mg0.165Mg3Al0.33Si3.67O10(OH)2			121.365	212.531	125.691	95.186	9.670
H-Nontronite	H0.33Fe2Al0.33Si3.67O10(OH)2			125.832	209.243	118.136	109.643	8.538
Na-Nontronite	Na0.33Fe2Al0.33Si3.67O10(OH)2			127.120	210.757	119.975	109.090	9.015
K-Nontronite	K0.33Fe2Al0.33Si3.67O10(OH)2			128.106	214.220	120.017	109.711	8.683
Ca-Nontronite	Ca0.165Fe2Al0.33Si3.67O10(OH)2			125.813	209.746	118.889	108.462	8.796
Mg-Nontronite	Mg0.165Fe2Al0.33Si3.67O10(OH)2			125.238	208.558	118.643	108.570	8.782
H-Montmorillonite	H0.33Mg0.33Al1.67Si4O10(OH)2			118.143	206.141	120.127	96.213	11.982
Na-Montmorillonite	Na0.33Mg0.33Al1.67Si4O10(OH)2			119.438	207.655	121.965	95.660	12.459
K-Montmorillonite	K0.33Mg0.33Al1.67Si4O10(OH)2			120.404	211.117	122.008	96.280	12.127
Ca-Montmorillonite	Ca0.165Mg0.33Al1.67Si4O10(OH)2			118.126	206.644	120.879	95.031	12.240
Mg-Montmorillonite	Mg0.495Al1.67Si4O10(OH)2			117.557	205.456	120.633	95.140	12.226
Low Fe-Mg Smectite	see below			124.488	212.196	125.025	96.544	11.228
High Fe-Mg Smectite	see below			125.565	209.115	127.383	95.619	11.088
Reykjanes Smectite	see below			129.117	215.785	130.929	94.535	11.213

Low Fe-Mg Smectite = Na0.15K0.2Ca0.02(Mg0.9Fe(+++)0.16Fe(++)0.29Al)(Al0.25Si3.75)O10(OH)2
Fe-Mg Smectite = Na0.1K0.2Ca0.025(Mg1.15Fe(+++)0.2Fe(++)0.5Al0.75)(Al0.5Si3.5)O10(OH)2
Reykjanes Smectite = Na0.33K0.03Ca0.66(Mg1.29Fe(+++)0.35Fe(++)0.33Mn0.01Al0.28)(Al0.83Si3.17)O10(OH)2

Table 13. Estimated Thermodynamic Data for 23 Smectite Compositions with interlayer hydration number of 5. The data in Table 4 for interlayer water properties are used along with the data for the corresponding dehydrated compositions from Table 8.

Name	Formula	$\Delta G_f°$ cal/mol	$\Delta H_f°$ cal/mol	S° cal/mol-K	V° cm^3/mol	a cal/mol-K	b x 10^3 cal/mol-K^2	c x 10^{-5} cal-K/mol
H-Beidellite	H0.33Al2Al0.33Si3.67O10(OH)2			123.386	212.175	126.658	100.033	12.879
Na-Beidellite	Na0.33Al2Al0.33Si3.67O10(OH)2			124.681	213.690	128.497	99.480	13.356
K-Beidellite	K0.33Al2Al0.33Si3.67O10(OH)2			125.646	217.152	128.539	100.101	13.024
Ca-Beidellite	Ca0.165Al2Al0.33Si3.67O10(OH)2			123.368	212.678	127.411	98.852	13.136
Mg-Beidellite	Mg0.165Al2Al0.33Si3.67O10(OH)2			122.800	211.491	127.165	98.960	13.123
H-Saponite	H0.33Mg3Al0.33Si3.67O10(OH)2			128.527	221.825	129.706	102.429	8.937
Na-Saponite	Na0.33Mg3Al0.33Si3.67O10(OH)2			129.821	223.340	131.545	101.876	9.414
K-Saponite	K0.33Mg3Al0.33Si3.67O10(OH)2			130.789	226.802	131.587	102.497	9.082
Ca-Saponite	Ca0.165Mg3Al0.33Si3.67O10(OH)2			128.510	222.328	130.459	101.248	9.194
Mg-Saponite	Mg0.165Mg3Al0.33Si3.67O10(OH)2			127.940	221.141	130.213	101.356	9.181
H-Nontronite	H0.33Fe2Al0.33Si3.67O10(OH)2			132.407	217.853	122.658	115.813	8.049
Na-Nontronite	Na0.33Fe2Al0.33Si3.67O10(OH)2			133.695	219.367	124.497	115.260	8.526
K-Nontronite	K0.33Fe2Al0.33Si3.67O10(OH)2			134.681	222.830	124.539	115.881	8.194
Ca-Nontronite	Ca0.165Fe2Al0.33Si3.67O10(OH)2			132.388	218.356	123.411	114.632	8.306
Mg-Nontronite	Mg0.165Fe2Al0.33Si3.67O10(OH)2			131.813	217.168	123.165	114.740	8.293
H-Montmorillonite	H0.33Mg0.33Al1.67Si4O10(OH)2			124.718	214.751	124.649	102.383	11.493
Na-Montmorillonite	Na0.33Mg0.33Al1.67Si4O10(OH)2			126.013	216.265	126.487	101.830	11.970
K-Montmorillonite	K0.33Mg0.33Al1.67Si4O10(OH)2			126.979	219.727	126.530	102.450	11.638
Ca-Montmorillonite	Ca0.165Mg0.33Al1.67Si4O10(OH)2			124.701	215.254	125.401	101.201	11.750
Mg-Montmorillonite	Mg0.495Al1.67Si4O10(OH)2			124.132	214.066	125.155	101.310	11.737
Low Fe-Mg Smectite	see below			131.063	220.806	129.547	102.714	10.739
High Fe-Mg Smectite	see below			132.140	217.725	131.905	101.789	10.598
Reykjanes Smectite	see below			135.692	224.395	135.451	100.705	10.723

Low Fe-Mg Smectite = Na0.15K0.2Ca0.02(Mg0.9Fe(+++)0.16Fe(++)0.29Al)(Al0.25Si3.75)O10(OH)2
Fe-Mg Smectite = Na0.1K0.2Ca0.025(Mg1.15Fe(+++)0.2Fe(++)0.5Al0.75)(Al0.5Si3.5)O10(OH)2
Reykjanes Smectite = Na0.33K0.03Ca0.66(Mg1.29Fe(+++)0.35Fe(++)0.33Mn0.01Al0.28)(Al0.83Si3.17)O10(OH)2

Table 14. Estimated Thermodynamic Data for 23 Smectite Compositions with interlayer hydration number of 7. The data in Table 4 for interlayer water properties are used along with the data for the corresponding dehydrated compositions from Table 8.

Name	Formula	$\Delta G_f°$ cal/mol	$\Delta H_f°$ cal/mol	S° cal/mol-K	V° cm^3/mol	a cal/mol-K	b x 10^3 cal/mol-K^2	c x 10^{-5} cal-K/mol
H-Beidellite	H0.33Al2Al0.33Si3.67O10(OH)2			149.686	246.615	144.746	124.713	10.921
Na-Beidellite	Na0.33Al2Al0.33Si3.67O10(OH)2			150.981	248.130	146.585	124.160	11.398
K-Beidellite	K0.33Al2Al0.33Si3.67O10(OH)2			151.946	251.592	146.627	124.781	11.066
Ca-Beidellite	Ca0.165Al2Al0.33Si3.67O10(OH)2			149.668	247.118	145.499	123.532	11.178
Mg-Beidellite	Mg0.165Al2Al0.33Si3.67O10(OH)2			149.100	245.931	145.253	123.640	11.165
H-Saponite	H0.33Mg3Al0.33Si3.67O10(OH)2			154.827	256.265	147.794	127.109	6.979
Na-Saponite	Na0.33Mg3Al0.33Si3.67O10(OH)2			156.121	257.780	149.633	126.556	7.456
K-Saponite	K0.33Mg3Al0.33Si3.67O10(OH)2			157.089	261.242	149.675	127.177	7.124
Ca-Saponite	Ca0.165Mg3Al0.33Si3.67O10(OH)2			154.810	256.768	148.547	125.928	7.236
Mg-Saponite	Mg0.165Mg3Al0.33Si3.67O10(OH)2			154.240	255.581	148.301	126.036	7.223
H-Nontronite	H0.33Fe2Al0.33Si3.67O10(OH)2			158.707	252.293	140.746	140.493	6.091
Na-Nontronite	Na0.33Fe2Al0.33Si3.67O10(OH)2			159.995	253.807	142.585	139.940	6.568
K-Nontronite	K0.33Fe2Al0.33Si3.67O10(OH)2			160.981	257.270	142.627	140.561	6.236
Ca-Nontronite	Ca0.165Fe2Al0.33Si3.67O10(OH)2			158.688	252.796	141.499	139.312	6.348
Mg-Nontronite	Mg0.165Fe2Al0.33Si3.67O10(OH)2			158.113	251.608	141.253	139.420	6.335
H-Montmorillonite	H0.33Mg0.33Al1.67Si4O10(OH)2			151.018	249.191	142.737	127.063	9.535
Na-Montmorillonite	Na0.33Mg0.33Al1.67Si4O10(OH)2			152.313	250.705	144.575	126.510	10.012
K-Montmorillonite	K0.33Mg0.33Al1.67Si4O10(OH)2			153.279	254.167	144.618	127.130	9.680
Ca-Montmorillonite	Ca0.165Mg0.33Al1.67Si4O10(OH)2			151.001	249.694	143.489	125.881	9.792
Mg-Montmorillonite	Mg0.495Al1.67Si4O10(OH)2			150.432	248.506	143.243	125.990	9.779
Low Fe-Mg Smectite	see below			157.363	255.246	147.635	127.394	8.781
High Fe-Mg Smectite	see below			158.440	252.165	149.993	126.469	8.640
Reykjanes Smectite	see below			161.992	258.835	153.539	125.385	8.765

Low Fe-Mg Smectite = Na0.15K0.2Ca0.02(Mg0.9Fe(+++)0.16Fe(++)0.29Al)(Al0.25Si3.75)O10(OH)2
Fe-Mg Smectite = Na0.1K0.2Ca0.025(Mg1.15Fe(+++)0.2Fe(++)0.5Al0.75)(Al0.5Si3.5)O10(OH)2
Reykjanes Smectite = Na0.33K0.03Ca0.66(Mg1.29Fe(+++)0.35Fe(++)0.33Mn0.01Al0.28)(Al0.83Si3.17)O10(OH)2

Table 15. Estimated Thermodynamic Data for 23 Smectite Compositions with implicit hydration (corresponding to unit water activity). At the present time, only Gibbs energy data are available.

Name	Formula	$\Delta G_f°$ cal/mol	$\Delta H_f°$ cal/mol	S° cal/mol-K	V° cm^3/mol	a cal/mol-K	b x 10^3 cal/mol-K^2	c x 10^{-5} cal-K/mol
H-Beidellite	H0.33Al2Al0.33Si3.67O10(OH)2	-1269753.6						
Na-Beidellite	Na0.33Al2Al0.33Si3.67O10(OH)2	-1279700.1						
K-Beidellite	K0.33Al2Al0.33Si3.67O10(OH)2	-1281785.7						
Ca-Beidellite	Ca0.165Al2Al0.33Si3.67O10(OH)2	-1280921.1						
Mg-Beidellite	Mg0.165Al2Al0.33Si3.67O10(OH)2	-1277076.6						
H-Saponite	H0.33Mg3Al0.33Si3.67O10(OH)2	-1324619.1						
Na-Saponite	Na0.33Mg3Al0.33Si3.67O10(OH)2	-1343891.1						
K-Saponite	K0.33Mg3Al0.33Si3.67O10(OH)2	-1345976.7						
Ca-Saponite	Ca0.165Mg3Al0.33Si3.67O10(OH)2	-1345112.1						
Mg-Saponite	Mg0.165Mg3Al0.33Si3.67O10(OH)2	-1341267.6						
H-Nontronite	H0.33Fe2Al0.33Si3.67O10(OH)2	-1056205.6						
Na-Nontronite	Na0.33Fe2Al0.33Si3.67O10(OH)2	-1075477.6						
K-Nontronite	K0.33Fe2Al0.33Si3.67O10(OH)2	-1077563.2						
Ca-Nontronite	Ca0.165Fe2Al0.33Si3.67O10(OH)2	-1076698.6						
Mg-Nontronite	Mg0.165Fe2Al0.33Si3.67O10(OH)2	-1072854.1						
H-Montmorillonite	H0.33Mg0.33Al1.67Si4O10(OH)2	-1255040.0						
Na-Montmorillonite	Na0.33Mg0.33Al1.67Si4O10(OH)2	-1274312.0						
K-Montmorillonite	K0.33Mg0.33Al1.67Si4O10(OH)2	-1276397.6						
Ca-Montmorillonite	Ca0.165Mg0.33Al1.67Si4O10(OH)2	-1275533.0						
Mg-Montmorillonite	Mg0.495Al1.67Si4O10(OH)2	-1271688.5						
Low Fe-Mg Smectite	see below	-1272667.3						
High Fe-Mg Smectite	see below	-1227165.4						
Reykjanes Smectite	see below	-1325017.9						

Low Fe-Mg Smectite = Na0.15K0.2Ca0.02(Mg0.9Fe(+++)0.16Fe(++)0.29Al)(Al0.25Si3.75)O10(OH)2
Fe-Mg Smectite = Na0.1K0.2Ca0.025(Mg1.15Fe(+++)0.2Fe(++)0.5Al0.75)(Al0.5Si3.5)O10(OH)2
Reykjanes Smectite = Na0.33K0.03Ca0.66(Mg1.29Fe(+++)0.35Fe(++)0.33Mn0.01Al0.28)(Al0.83Si3.17)O10(OH)2

Table 16. Entropies of the Elements in Their Reference Forms, Compiled from Various Sources. The list here addresses only elements of interest in relation to clay minerals. Colors correspond to sources. Values adopted here are given on the right hand side.

Elemental Reference Entropies (S°)

	NBS 1982	CODATA 1989	NEA 1992-	Barin 1995		Used Here	Used Here
Element	J/mol-K	J/mol-K	J/mol-K	J/mol-K	Element	J/mol-K	cal/mol-K
Al	28.33	28.30	28.300	28.275	Al	28.300	6.764
Ba	62.8	-----	62.420	62.417	Ba	62.420	14.919
Ca	41.42	41.59	41.590	41.422	Ca	41.590	9.940
Cs	85.23	85.23	85.230	85.147	Cs	85.230	20.370
F	101.39	101.3955	101.3955	101.3975	F	101.3955	24.234
Fe	27.28	-----		27.280	Fe	27.280	6.520
H	65.342	65.340	65.340	65.340	H	65.340	15.617
K	64.18	64.68	64.680	64.670	K	64.680	15.459
Li	29.12	29.12	29.120	29.080	Li	29.120	6.960
Mg	32.68	32.67	32.670	32.677	Mg	32.670	7.808
Mn	32.01	-----		32.008	Mn	32.008	7.650
Na	51.21	51.30	51.300	51.455	Na	51.300	12.261
O	102.569	102.576	102.576	102.5735	O	102.576	24.516
Ra	71	-----		-----	Ra	71	16.969
Rb	76.78	76.78	76.780	76.780	Rb	76.780	18.351
Si	18.83	18.81	18.810	18.820	Si	18.810	4.496
Sr	52.3	-----	55.700	55.690	Sr	55.700	13.313

For future work, we intend to obtain and analyze additional data to construct more accurate estimates of the thermodynamic properties of complex clays, with a focus on hydration/dehydration and ion exchange. We intend to carry forward the implicitly hydrated model as at least a point of comparison. However, the main goal of present and future work is to develop a corresponding model that explicitly treats the interlayer water and covers states of variable hydration and which reasonably explains a wide variety of types of physical measurements, including thermogravimetry and XRD studies of dehydration, ion exchange measurements, solubilities, and swelling pressures. We also intend to work in such insight as is possible from molecular dynamics studies (e.g., Cygan et al., 2004). The goal here would be do develop data for end-member compositions such as $Na_{0.33}Al_2Al_{0.33}Si_{3.67}O_{10}(OH)_2.n\ H_2O$, where n is likely to have a maximum value between 4.5 and 7, and to appropriately describe the thermodynamics of mixing.

Ransom and Helgeson (1993, 1994ab, 1995) developed an approach to deal with variable hydration. It has some excellent features. However, it does not extend to a complete treatment of smectite thermodynamics in that it does not develop estimates of Gibbs energies for the various end member compositions that are discussed. Rather, it only addresses Gibbs energies of dehydration between fully hydrated and dehydrated end-members of otherwise fixed composition. It doesn't cover the full range of clay mineral compositions that is desired. Also, it leaves open some questions as to how to handle hydration/dehydration when that depends on the interlayer cation content, which can be quite variable. In their 1995 paper, they make an attempt at modeling the case of mixed Na and Ca in the interlayer, but this aspect was insufficiently developed and tested. Nevertheless, their model does show a path forward to extending the Tardy-Garrels type model thus far developed.

Tardy and Duplay (1992) go farther than Ransom and Helgeson (papers cited above) in that they address both interlayer water and the full thermodynamic stability of end-member clay compositions. Their approach provides a counterpoint to both aspects of the model we are working to develop, and various parts of their model may simply be incorporated into ours. Some papers by Viellard (1994ab, 2000) are also of interest in this regard (his 2000 paper addresses interlayer water). Vidal and Dubacq (2011) have recently proposed a model for interlayer water and full stability that is also of great interest. Work that remains to be done is to compare and evaluate these models, as they have different ranges of focus and often have implications beyond what is addressed directly. There are, for example, implications of these models to high temperature ion exchange and swelling pressure behavior that are not fully developed or explored. This is a reflection of the complexity of the topic area. There appears to have been only rather limited penetration of such models into geochemical modeling and reactive transport simulation. In fact, there seem to be few computational tools available to readily assess the consequences of these models.

In summary, this remains a work in process. Together with our SNL collaborator, Carlos Jove-Colon, we will improve the existing data/models for complex clays by:

- Explicitly accounting for water in the exchange layers of smectites and vermiculites
- Accounting for a broader spectrum of physical measurements (e.g., basal spacing studies of clay dehydration, swelling pressure data, ion exchange data over a wide range of temperature)
- Including insights from molecular dynamics (MD) modeling regarding dehydration (in part via informal collaboration with R. Cygan's MD modeling group at SNL).
- Developing computational tools to evaluate existing and new models.

References

Barin, I. and Platzki, G. 1995. *Thermochemical Data of Pure Substances.* 3rd Edition. Two volumes. New York, New York: VCH Publishers.

Binnewies, M. and Milke, E. 1999. *Thermochemical Data of Elements and Compounds.* New York, New York: Wiley-VCH.

BSC (Bechtel SAIC Company) 2007a. *Qualification of Thermodynamic Data for Geochemical Modeling of Mineral–Water Interactions in Dilute Systems*. ANL-WIS-GS-000003 REV 01. Las Vegas, Nevada: Bechtel SAIC Company. DOC.20070619.0007.

BSC (Bechtel SAIC Company) 2007b. *In-Drift Precipitates/Salts Model*. ANL-EBS-MD-000045 REV 03. Las Vegas, Nevada: Bechtel SAIC Company. DOC.20070306.0037.

Fu, M.H., Zhang, Z.Z. and Low, P.F. 1990. "Changes in the properties of a montmorillonite-water system during the adsorption and desorption of water: hysteresis." *Clays and Clay Minerals*, 38, 485-492.

Cox, J.D.; Wagman, D.D.; and Medvedev, V.A., eds. 1989. *CODATA Key Values for Thermodynamics.* CODATA Series on Thermodynamic Values. New York, New York: Hemisphere Publishing Company.

Cygan, R.T., Liang, J.-J., and Kalinichev, A.G. 2004. "Molecular Models of Hydroxide, Oxyhydroxide, and Clay Phases and the Development of a General Force Field." *Journal of Physical Chemistry B* 108, 1255-1266.

Deer, W.A., Howie, R.A., and Zusman, J. 1962. *Rock-Forming Minerals. Vol. 3, Sheet Silicates*. Longmans, London. 270 p.

Garrels, R.M., and Christ, C.L. 1965 *Solutions, Minerals, and Equilibria*. Boston, Massachusetts: Jones and Bartlett Publishers

Greenberg, J.P. and Moller, N. 1989. “The Prediction of Mineral Solubilities in Natural Waters: A Chemical Equilibrium Model for the Na-K-Ca-Cl-SO_4-H_2O System to High Concentration from 0 to 250°C.” *Geochimica et Cosmochimica Acta* 53, 2503–2518.

Grenthe, I., Fuger, J., Konings, R.J.M., Lemire, R.J., Muller, A.B., Nguyen-Trung, C., and Wanner, H. 1992. *Chemical Thermodynamics of Uranium. Volume 1 of Chemical Thermodynamics.* Wanner, H. and Forest, I., eds. Amsterdam, The Netherlands: North-Holland Publishing Company.

Helgeson, H.C. 1969. “Thermodynamics of Hydrothermal Systems at Elevated Temperatures and Pressures.” American Journal of Science, 267(6), 729-804.

Helgeson, H.C.; Delany, J.M.; Nesbitt, H.W.; and Bird, D.K. 1978. “Summary and Critique of the Thermodynamic Properties of Rock Forming Minerals.” *American Journal of Science, 278-A.* New Haven, Connecticut: Yale University, Kline Geology Laboratory.

Johnson, J.W.; Oelkers, E.H.; and Helgeson, H.C. 1992. “SUPCRT92: A Software Package for Calculating the Standard Molal Thermodynamic Properties of Minerals, Gases, Aqueous Species, and Reactions from 1 to 5000 Bar and 0 to 1000°C.” *Computers & Geosciences, 18,* (7), 899-947. New York, New York: Pergamon Press.

Liu, C.-W., and Lin, W.-S. 2005. “A Smectite Dehydration Model in a Shallow Sedimentary Basin: Model Development.” *Clays and Clay Minerals*, 53, 55-70.

Pabalan, R.T. and Pitzer, K.S. 1987. “Thermodynamics of Concentrated Electrolyte Mixtures and the Prediction of Mineral Solubilities to High Temperatures for Mixtures in the System Na-K-Mg-Cl-SO4-OH-H2O.” *Geochimica et Cosmochimica Acta*, 51(9), 2429-2443

Parker, V.B. and Khodakovskii, I.L. 1995. “Thermodynamic Properties of the Aqueous Ions (2+ and 3+) of Iron and the Key Compounds of Iron.” *Journal of Physical and Chemical Reference Data, 24,* (5), 1699-1745. Washington, D.C.: American Chemical Society.

Pitzer, K.S. 1991. “Ion Interaction Approach: Theory and Data Correlation.”Chapter 3 of *Activity Coefficients in Electrolyte Solutions*. 2nd Edition. Pitzer, K.S.,ed. Boca Raton, Florida: CRC Press.

Ransom, B. and Helgeson, H.C. 1993. “Compositional End Members and Thermodynamic Components of Illite and Dioctahedral Aluminous Smectite Solid Solutions.” *Clays and Clay Minerals* 41(5), 537-550.

Ransom, B. and Helgeson, H.C. 1994a. “Estimation of the Standard Molal Heat Capacities, Entropies, and Volumes of 2:1 Clay Minerals.” *Geochimica et Cosmochimica Acta*, 58 (21), 4537-4547.

Ransom, B. and Helgeson, H.C. 1994b. “A Chemical and Thermodynamic Model o f Aluminous Dioctahedral 2:1 Layer Clay Minerals in Diagenetic Processes: Regular Solution

Representation of Interlayer Dehydration in Smectite." *American Journal of Science* 294, 449-484.

Ransom, B. and Helgeson, H.C. 1995. "A Chemical and Thermodynamic Model o f Aluminous Dioctahedral 2:1 Layer Clay Minerals in Diagenetic Processes: Dehydration of Dioctahedral Aluminous Smectite as a Function of Temperature and Depth in Sedimentary Basins." *American Journal of Science* 295, 245-281.

Robie, R.A., and Hemingway, B.S. 1995. *Thermodynamic Properties of Minerals and Related Substances at 298.15 K and 1 Bar (10^5 Pascals) Pressure and at Higher Temperatures.* Bulletin 2131. Reston, Virginia: U.S. Geological Survey.

Tamura, K., Yamada, H., and Nakazawa, H. 2000. "Stepwise Hydration of High-Quality Synthetic Smectite with Various Cations." *Clays and Clay Minerals* 48, 400-404.

Tardy, Y., and Garrels, R.M. 1974. "A Method of Estimating the Gibbs Energies of Formation of Layer Silicates." *Geochimica et Cosmochimica Acta* 38(7), 1101-1116.

Tardy, Y., and Duplay, J. 1992. "A Method of Estimating the Gibbs Free Energies of Formation of Hydrated and Dehydrated Clay Minerals." *Geochimica et Cosmochimica Acta* 56(16), 3007-3029

Valenzuela Díaz, F.R., and de Souza Santos, P. 2001. "Studies on the Acid Activation of Brazilian Smectite Clays." Química Nova 24(3), 345-353.

Vidal, O., and Dubacq, B. 2009. "Thermodynamic modeling of clay dehydration, stability and compositional evolution with temperature, pressure and H_2O activity." *Geochimica et Cosmochimica Acta* 73, 6544-6564.

Vieillard, P. 1994a. "Prediction of Enthalpy of Formation Based on Refined Crystal Structures of Multisite Compounds: Part 1. Theories and Examples." *Geochimica et Cosmochimica Acta* 58(19), 4049-4063.

Vieillard, P. 1994b. "Prediction of Enthalpy of Formation Based on Refined Crystal Structures of Multisite Compounds: Part 2. Application to Minerals Belonging to the System Li_2O-Na_2O-K_2O-BeO-MgO-CaO-MnO-FeO-Fe_2O_3-Al_2O_3-SiO_2-H_2O. Results and Discussion." *Geochimica et Cosmochimica Acta*, 58(19), 4065-4107.

Vieillard, P. 2000. "A New Method for the Prediction of Gibbs Free Energies of Formation of Hydrated Clay Minerals Based on the Electronegativity Scale." *Clay and Clay Minerals,* 48(4), 459-473.

Wagman, D.D.; Evans, W.H.; Parker, V.B.; Schumm, R.H.; Halow, I.; Bailey, S.M.; Churney, K.L.; and Nuttall, R.L. 1982. "The NBS Tables of Chemical Thermodynamic Properties, Selected Values for Inorganic and C_1 and C_2 Organic Substances in SI Units." *Journal of*

Physical and Chemical Reference Data, *11*, (Supplement No. 2), 2-276 - 2-282. Washington, D.C.: American Chemical Society.

Wagman, D.D.; Evans, W.H.; Parker, V.B.; Schumm, R.H.; Halow, I.; Bailey, S.M.; Churney, K.L.; and Nuttall, R.L. 1989. "Erratum: The NBS Tables of Chemical Thermodynamic Properties, Selected Values for Inorganic and C_1 and C_2 Organic Substances in SI Units." *Journal of Physical and Chemical Reference Data*, *18*, (4), 2-276 - 2-282, 1807-1812. Washington, D.C.: American Chemical Society.

Wang, Y., Simpson, M., Painter, S., Liu, H.-H., and Kersting, A.B. 2011. *Natural System Evaluation and Tool Development – FY11 Progress Report*: Fuel Cycle Research and Development. Document FCRD-USED-2011-000223 (originated from Sandia National Laboratories).

Wolery, T.J. 1978. Some Chemical Aspects of Hydrothermal Processes at Mid-Oceanic Ridges - A Theoretical Study. I. Basalt-Sea Water Reaction and Chemical Cycling Between the Oceanic Crust and the Oceans. II. Calculation of Chemical Equilibrium Between Aqueous Solutions and Minerals. Ph.D. dissertation. Evanston, Illinois: Northwestern University.

Xiong, Y.-L. 2005. "Release of FMT-050405.CHEMDAT."E-mail to J.F. Kanney and J.J. Long, April 5, 2005. Carlsbad, NM: Sandia National Laboratories. ERMS 539304.